

Electromagnetic probes in heavy-ion collisions

Messengers from the hot and dense phase

H. van Hees^{1,2,a}, J. Weil^{2,b}, S. Endres^{2,c}, and M. Bleicher^{2,d}

¹*Johann Wolfgang Goethe University Frankfurt, Institute for Theoretical Physics, Max-von-Laue-Str. 1, 60438 Frankfurt, Germany*

²*Frankfurt Institute of Advanced Studies, Ruth-Moufang-Str. 1, 60438 Frankfurt, Germany*

Abstract. Due to their penetrating nature, electromagnetic probes, i.e., lepton-antilepton pairs (dileptons) and photons are unique tools to gain insight into the nature of the hot and dense medium of strongly-interacting particles created in relativistic heavy-ion collisions, including hints to the nature of the restoration of chiral symmetry of QCD. Of particular interest are the spectral properties of the electromagnetic current-correlation function of these particles within the dense and/or hot medium. The related theoretical investigations of the in-medium properties of the involved particles in both the partonic and hadronic part of the QCD phase diagram underline the importance of a proper understanding of the properties of various hadron resonances in the medium.

1 Introduction

The transverse-momentum and invariant-mass spectra of the so-called electromagnetic probes, i.e., dileptons (e^+e^- or $\mu^+\mu^-$ pairs) and photons have been identified as interesting observables early on [1]. Since they do not participate in the strong interaction, they leave the hot and dense fireball created in ultrarelativistic heavy-ion collisions nearly undisturbed by final-state interactions and thus provide a direct insight into the spectral properties of the electromagnetic current-current correlation function in the medium during the entire evolution of the collision. For theory this is also some challenge since an accurate description of the invariant-mass spectra of dileptons and transverse-momentum spectra of both dileptons and photons is needed, including as comprehensive a set of sources as possible, reaching from the radiation from the very early stage of the collision (Drell-Yan processes) over the emission from a hot and dense partonic medium (Quark-Gluon Plasma, QGP) undergoing the transition to a hot and dense hadron-resonance gas (which is close to the chemical freeze-out of the medium), to the finally decoupled hadronic state at thermal freeze-out.

In this paper we summarize the current status of our understanding of both the spectral properties of the electromagnetic current-correlation function, implying some insights about the nature of chiral-symmetry restoration, and the description of the evolution of the hot and dense partonic and hadronic fireball.

^ae-mail: hees@fias.uni-frankfurt.de

^be-mail: weil@fias.uni-frankfurt.de

^ce-mail: endres@th.physik.uni-frankfurt.de

^de-mail: bleicher@th.physik.uni-frankfurt.de

After a brief review in Sec. 2 about how to model the main thermal sources of electromagnetic probes in heavy-ion collisions, in Sec. 3 we turn to a short description of various models for the evolution of the hot and dense fireball. Finally in Sec. 4 we present the comparison of these models to recent data from the HADES (GSI), NA60 (CERN SPS), and STAR (RHIC) collaborations and give and outlook to what to expect from future experiments at FAIR and LHC.

2 Sources of dileptons and photons

Phenomenologically, at not too low collision energies the medium created in heavy-ion collisions is well described as a collectively expanding fluid in terms of hydrodynamical models [2–5]. This implies that it is close to local thermal equilibrium over a large part of its evolution. This suggests that models for the production of electromagnetic probes, based on relativistic many-body quantum field theory (for reviews cf. [6, 7]) are applicable.

Generally the radiation of photons and dileptons (“virtual photons”) are given in terms of the retarded electromagnetic current-current correlation function,

$$\Pi_{\text{em}}^{\mu\nu}(q_0, q) = -i \int d^4x e^{iq \cdot x} \Theta(x_0) \left\langle \left[\hat{j}_{\text{em}}^\mu(x), \hat{j}_{\text{em}}^\nu(0) \right] \right\rangle. \quad (1)$$

For dileptons the invariant rate reads [8, 9]

$$\frac{dN_{ll}}{d^4x d^4q} = -\frac{\alpha_{\text{em}}^2}{\pi^3 M^2} f_{\text{B}}(q_0; T) \frac{1}{3} g_{\mu\nu} \text{Im} \Pi_{\text{em}}^{\mu\nu}(M, q; \mu_{\text{B}}, T). \quad (2)$$

Here, $\alpha_{\text{em}} \simeq 1/137$ denotes the electromagnetic coupling constant, q_0 and q the energy and three-momentum of the lepton pair in the restframe of the fluid cell at space-time position x ; M is its invariant mass, μ_{B} the baryon-chemical potential, and T the temperature of the medium.

In the following we briefly review some models used to describe the em. current correlation function of strongly interacting matter. In the vacuum, the corresponding spectral function (1) is empirically given by the cross section for the reaction $e^+ + e^- \rightarrow \text{hadrons}$ [10]. In the low-mass range $M \lesssim 1$ GeV it shows the low-lying vector-meson resonances, ρ , ω , and ϕ and in the intermediate-mass range ($1 \text{ GeV} \lesssim M \lesssim 3 \text{ GeV}$) a continuum. In pp and AA collisions also the Dalitz decays of the π^0 and η Dalitz decays are prominent sources of dileptons.

2.1 Thermal radiation from a QGP

To lowest order the dominant dilepton-production process is the purely electromagnetic annihilation of a quark-anti-quark pair to an $\ell^+ \ell^-$ pair. The in-medium properties of the corresponding production rate have been described using the leading-order hard-thermal-loop formalism of thermal QCD [11] and more recently at complete next-to-leading order, including a resummation taking the Landau-Pomeranchuk-Migdal effect into account [12] close to the light cone, $q^0 = q$. Also results from lattice-QCD calculations [13, 14] are available and have been extrapolated to finite three-momentum in [15] and found in fair agreement with the microscopic QCD description.

2.2 Thermal radiation from a hadron-resonance gas

At lower temperatures and densities, the in-medium current-correlation functions have to be addressed using effective hadronic models. One quite model-independent way is to use the corresponding empirical vacuum spectral functions and low-density approximations to evaluate its medium modifications or to employ so-called “chiral reduction schemes” [16–18].

Beyond this leading-order low-density methods a detailed effective hadronic model is necessary to evaluate reliable in-medium spectral functions, including its three-momentum dependence. Starting from the observation that the vector-meson dominance (VMD) model, i.e., the assumption that the hadronic electromagnetic current is proportional to the fields of the low-lying vector-meson resonances, ρ , ω , and ϕ , provide a good description of the vacuum cross section, various effective hadronic models have been developed, e.g., [6, 19] and carefully fitted to the corresponding data in “elementary reactions” like dilepton production in pp collisions or photon-absorption data on nucleons and nuclei. Within such empirical constraints the resulting dilepton-production rates based on the evaluation of these models at finite temperature and/or density are in satisfying agreement with each other.

According to these models medium modifications are due to two major effects: (a) the medium modification of the pion cloud, i.e., the dressing of, e.g., the pion loop in the ρ -meson self-energy diagram due to hadronic interactions of the pions with the medium and (b) the direct interaction of the vector mesons with mesons and baryons, including a variety of resonance states. Both self-energy diagrams need a proper dressing of the corresponding vertex functions to guarantee electromagnetic gauge invariance. Besides the interactions with the nucleon and $\Delta(1232)$ also heavier baryon resonances like the $N(1440)$, $N(1520)$, $N(1535)$, $\Delta(1700)$, etc. play an important role. These interactions lead to a tremendous broadening of the vector-meson spectral functions with quite moderate mass shifts. This can be explained by the fact that any interaction process leads to an increase of the imaginary part of the retarded self-energy (“collisional broadening”) while its real part is lowered or raised depending on the attractive or repulsive nature of the interaction. It is important to note that also in heavy-ion collisions at the highest available energies the interaction of the vector mesons with baryons are the dominating source of these medium modifications, although the net-baryon number (baryon-chemical potential) is low in this case. The reason is that, due to the CP invariance of the strong interaction, baryons and antibaryons add in the same way to the medium modifications of the vector mesons, i.e., the relevant quantity is not the net-baryon number density, $n_B - n_{\bar{B}}$ but the total one, $n_B + n_{\bar{B}}$.

In addition, in the intermediate-mass region also contributions from multi-pion processes (like $a_1, \omega + \pi$ reactions) are implemented via low-density approximations, including vector-axial-vector mixing [20], using the empirical vacuum spectra of the vector- and axial-vector current-correlation function from τ -decay data [21, 22].

3 Fireball-evolution models

Having good models for the in-medium properties of the electromagnetic current-correlation function at hand, as a second ingredient for a realistic description of dilepton production in heavy-ion collisions also a reliable model for the evolution of the partonic and hadronic bulk medium is necessary, since the dilepton (and photon) spectra are given by the integral of the corresponding rate (2) over the entire space-time four volume of the fireball during its whole lifetime. While the integrated invariant-mass dilepton spectrum is a Lorentz-invariant quantity, for the transverse-momentum spectra the (radial) flow-velocity field of the medium becomes important due to the corresponding Doppler-blue shift of the spectra of the irradiated photons or dileptons [21–24]. The description of the collective fireball dynamics reaches from simple blastwave fireball parameterizations [21, 22, 24] over hydrodynamical models [23, 25–27] to detailed transport and “hybrid” transport-hydrodynamics models [28–33].

One problem with the transport approach is the difficulty to implement medium effects consistently. While the implementation of vacuum cross sections and decay rates of hadrons into dileptons and photons is quite straight forward, the medium modifications of such processes should, in principle, be calculated within the same off-equilibrium setup as in the corresponding kinetic description implemented in the transport models, including the proper treatment of “off-shell transport prescriptions”.

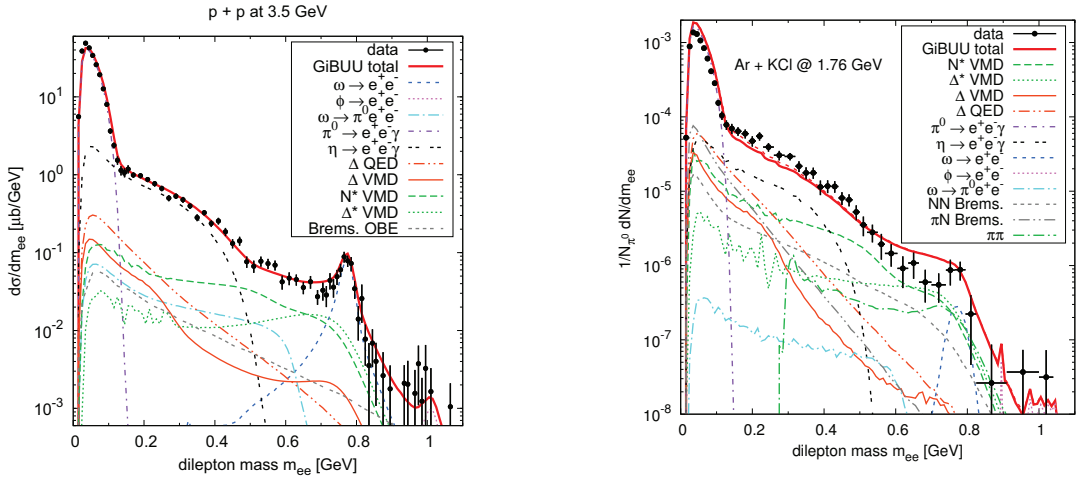


Figure 1. Comparison of the dilepton invariant-mass spectrum from the GiBUU transport model in 3.5 GeV pp (left) and 1.76A GeV Ar-KCl collisions with data from the HADES collaboration [38, 39].

However this is out of reach with present methods. Thus, more recently, a coarse-graining prescription has been used to make the equilibrium-quantum-field-theory results for the thermal dilepton/photon rates applicable within the underlying transport model for the bulk evolution [34–37] (see also S. Endres’s contribution to these proceedings [37]).

4 Heavy-ion collisions at various energies

In this Section we present the comparison of some of the contemporary models for dilepton production to recent data, covering an energy range from $\sim 1A$ GeV (SIS at GSI) to top RHIC energy of 200A GeV.

4.1 GSI and future FAIR experiments

We start our comparison of the above summarized modeling of dileptons to recent heavy-ion collision data with the measurements by the HADES collaboration at the GSI SIS [38, 39]. One of the motivations to take data at low collision energies was the verification of previous data in this collision-energy range by the DLS collaboration, which have shown a large enhancement of the dilepton yield in the low-mass region. The HADES measurement confirmed this finding, providing a challenge for theory.

As an example, in Fig. 1 we compare the results from the GiBUU transport model [32, 40–43] with the data from 3.5 GeV pp and 1.76A GeV Ar+KCl collisions from the HADES collaboration [38, 39]. The model implements an extension of the baryon-resonance model described in [19] into the GiBUU transport simulation. The model parameters (resonance masses, widths, and coupling constants) are fit to the partial-wave analysis by Manley and Saleski [44]. The coupling to the electromagnetic sector is based on a strict VMD model, i.e., all dileptons are produced via an intermediate light vector meson. This can be interpreted as a specific model for the hadronic electromagnetic transition form factors in

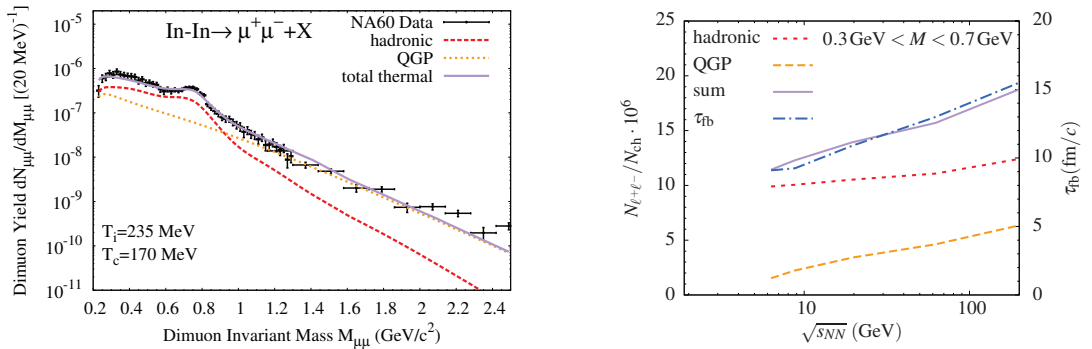


Figure 2. Left: Invariant-mass spectrum with a simple blastwave thermal fireball model, using the medium-modified current correlation function of the Rapp-Wambach model in 158A GeV In+In collisions at the CERN SPS compared to acceptance corrected data from the NA60 collaboration [47, 48]. Right: Excitation function of the dilepton excess yield as a function of the center-mass beam energy in AA ($A \simeq 200$) collisions.

the Dalitz-decay cross sections for the baryon resonances, including the $\Delta(1232)$ ¹. The sensitivity of the transition form factor is illustrated in the left panel of Fig. 1, where the VMD-form factor model is compared to a pure electromagnetic (QED) coupling. The former provides a very satisfactory description of dielectron production in elementary reactions. Only at the lowest collision energies some discrepancies in comparison to the HADES data in np collisions (from a quasi-free scattering analysis in dp collisions) are found, which we trace back mostly to the difficulties to fully describe and implement the bremsstrahlung contributions within the transport-model approach [32]. The comparison of the model with the Ar+KCl data (right panel of Fig. 1) indicates the possible influence of some medium modifications of the ρ and ω meson: A broadening of their spectra should decrease the dilepton yield around the peak region, $M \simeq m_\rho \simeq 770$ MeV and enhance it at lower masses. The model also describes the measured transverse-mass (m_t) and rapidity (y) spectra satisfactorily. A first comparison with the Au-Au data, recently presented at the Quark Matter conference, also indicates the need for medium modifications of the vector-meson spectral functions.

Thus, we have also applied the coarse-graining approach to the UrQMD transport model [45] which enables us to use the hadronic many-body theory for thermal dilepton rates by Rapp and Wambach [46], which is based on a similar hadron-resonance model as the one used in the GiBUU transport model but evaluated at finite temperature and baryon-chemical potential. Applying the medium modified vector-meson spectral functions to the dilepton rates leads to an excellent description of both the Ar+KCl (for the invariant-mass as well as the m_t and y spectra) [45].

4.2 SPS, RHIC

In the SPS energy regime we can compare the models to the high-precision measurement of the dimuon excess spectrum by the NA60 collaboration in 158A GeV In+In collisions. Based on data, here the Dalitz-decay contributions at low masses, the yield from the decay of correlated $D\bar{D}$ pairs as well as from the hard Drell-Yan processes in the intermediate-mass region has been subtracted in a model-independent way and made available as acceptance corrected mass spectra (also in a comprehensive set of p_t bins). Here, a considerable contribution from the QGP phase as well as from

¹Due to the p-wave nature of the $\rho N\Delta$ - coupling, the impact on the hadronic properties of the $\Delta(1232)$ resonance are negligible [42].

multi-pion processes as described in Sec. 2 is necessary to describe the data in the intermediate-mass region. For the first time the accuracy of the data has been sufficient to distinguish model predictions of the dilepton spectra from hadronic-many-body theory, leading to a tremendous broadening of the light vector meson's spectral functions with small mass shifts, from those within a dropping-mass scenario based on predictions from a particular realization (vector manifestation) of chiral symmetry [49–52].

In addition, the slope of the acceptance-corrected invariant-mass spectrum provides an excellent measurement of a space-time averaged temperature of the dilepton source in this region, which is dominated by emission from the QGP phase of the fireball evolution. Note that this “invariant slope” is unaffected from the Doppler blue-shift effect due to radial flow, which is present in the corresponding slopes of the transverse-mass spectra. The temperature extracted by a fit to the NA60 invariant-mass spectrum, where the non-thermal contributions from the hard Drell-Yan process as well as from the decays of correlated $D\bar{D}$ mesons have been subtracted, $T_{M\text{-slope}} \approx 205\text{-}230$ MeV, is well above the pseudo-critical temperature of the confinement-deconfinement and chiral-symmetry (cross-over) phase transition of $T_c \approx 160$ MeV.

Both the implementation of the medium-modified dilepton rates within the coarse-graining approach with UrQMD [36, 37] and in a simple expanding fireball model (cf. left panel of Fig. 2) show an excellent agreement with the NA60 data. This also holds for the p_t -differential invariant-mass and the p_t spectra measured by the NA60 collaboration (see also S. Endres's contribution to these proceedings [37]). In addition, the same model for the in-medium modified current-correlation function of strongly interacting matter has been successfully employed to the dilepton measurement by the STAR collaboration² at RHIC [15] as well as the transverse-momentum spectra and elliptic-flow parameter, $v_2(p_t)$, of “direct photons” at RHIC and LHC [54–56]. The surprisingly high elliptic flow of the direct photons found at both RHIC and LHC underline the importance of realistic models for photon production in the hadronic phase, resulting in a dominant emission of photons from the phase of the medium around the pseudo-critical temperature, showing a considerable blue-shift effect in the effective slopes of the photon- p_t spectra. Both findings indicate an early buildup of both radial and elliptic flow. By comparison with hydrodynamic-model calculations for the bulk evolution it has also been demonstrated that simple blastwave-fireball parameterizations, constrained by hadronic freeze-out spectra (p_t and $v_2(p_t)$), are surprisingly reliable in describing both the dilepton and photon spectra, based on the same in-medium model for the electromagnetic current-correlation function. As shown above, this also holds for the description of the fireball dynamics with transport models as well as hybrid transport-hydro models.

5 Conclusions and outlook

These findings demonstrate that the electromagnetic probes (dileptons and photons) in heavy-ion collisions are quite well understood in terms of partonic and hadronic models for the medium modified electromagnetic current-correlation function. In the low-mass region, the invariant-mass spectra of dileptons show some sensitivity to the medium modifications of vector mesons, underlining the importance of reliable effective hadronic models, implementing the dynamics of a variety of meson and baryon resonances, which have to be well-constrained by empirical input on elementary cross sections. Here, the recent measurements of pion-induced reactions by the HADES collaboration at the GSI SIS are very promising for evaluating and improving these models in further detail, particularly in the low collision-energy region.

²The very large enhancement seen by the PHENIX collaboration [53] in the most central bin, cannot be described by the currently employed theoretical models.

The relative robustness of the electromagnetic probes to the details of the bulk evolution, together with high-precision measurements of the dilepton invariant-mass spectrum as well as p_t spectra and $v_2(p_t)$ of direct photons (and also dileptons in the near future) can also help to shed further light on the bulk-evolution properties. With simple fireball parameterizations it is quite easy to reliably predict both the invariant effective slope (and thus a space-time averaged true temperature, unaffected by blue-shift effects due to radial flow) and the life-time of the fireball, which is the only parameter to be adjusted to the overall dilepton or photon yield, as soon as the partonic and hadronic models for the in-medium production rates and the bulk-medium evolution model are fixed.

This enables us to make predictions of various “excitation functions” like the invariant-slope temperature, the dilepton excess yield in the low-mass region, and the fireball lifetime (cf. the right panel of Fig. 2) as a function of the center-mass beam energy, which is addressed currently in the beam-energy-scan program at RHIC and at the future CBM experiment at the FAIR project. The here shown excitation functions are based on an cross-over equation of state for all beam energies, constrained by lattice-QCD calculations [57]. Since at least the invariant-slope temperature is quite sensitive to the employed equation of state, the hope is to find indications for a change from a cross-over phase transition at higher beam energies (low baryon-chemical potential) to a first-order phase transition (higher baryon-chemical potentials) or maybe even the existence of a critical point in the QCD phase diagram. Via the invariant-slope temperature at least an indication for the transition from a fireball evolution starting in a partonic phase to one which is entirely of hadronic nature should be possible. In turn these alterations of the phase-transition behavior should also be reflected in the total lifetime of the fireball (“critical slowing down” close to a critical point) and the directly related overall yield of em. probes.

References

- [1] E.V. Shuryak, Phys. Lett. B **78**, 150 (1978)
- [2] D. Teaney, J. Lauret, E. Shuryak (2001), arXiv: nucl-th/0110037
- [3] T. Hirano, K. Tsuda, Phys. Rev. C **66**, 054905 (2002)
- [4] P.F. Kolb, U. Heinz (2003), published in R. C. Hwa, X.-N. Wang (Ed.), Quark Gluon Plasma 3, World Scientific
- [5] C. Nonaka, S.A. Bass, Phys. Rev. C **75**, 014902 (2007)
- [6] R. Rapp, J. Wambach, Adv. Nucl. Phys. **25**, 1 (2000)
- [7] R. Rapp, J. Wambach, H. van Hees, Landolt-Börnstein **I/23**, 4 (2009)
- [8] L.D. McLerran, T. Toimela, Phys. Rev. D **31**, 545 (1985)
- [9] C. Gale, J.I. Kapusta, Nucl. Phys. B **357**, 65 (1991)
- [10] K. Olive et al. (Particle Data Group), Chin. Phys. C **38**, 090001 (2014)
- [11] E. Braaten, R.D. Pisarski, T.C. Yuan, Phys. Rev. Lett. **64**, 2242 (1990)
- [12] I. Ghisoiu, M. Laine, JHEP **1410**, 83 (2014)
- [13] H.T. Ding, A. Francis, O. Kaczmarek, F. Karsch, E. Laermann et al., Phys. Rev. D **83**, 034504 (2011)
- [14] B.B. Brandt, A. Francis, H.B. Meyer, H. Wittig, JHEP **1303**, 100 (2013)
- [15] R. Rapp, Adv. High Energy Phys. **2013**, 148253 (2013)
- [16] V. Eletsky, M. Belkacem, P. Ellis, J.I. Kapusta, Phys. Rev. C **64**, 035202 (2001)
- [17] J.V. Steele, H. Yamagishi, I. Zahed, Phys. Lett. B **384**, 255 (1996)
- [18] J.V. Steele, H. Yamagishi, I. Zahed, Phys. Rev. D **56**, 5605 (1997)
- [19] S. Teis, W. Cassing, M. Effenberger, A. Hombach, U. Mosel et al., Z. Phys. A **356**, 421 (1997)

- [20] M. Dey, V.L. Eletsky, B.L. Ioffe, Phys. Lett. B **252**, 620 (1990)
- [21] H. van Hees, R. Rapp, Nucl. Phys. A **806**, 339 (2008)
- [22] H. van Hees, R. Rapp, Phys. Rev. Lett. **97**, 102301 (2006)
- [23] K. Dusling, D. Teaney, I. Zahed, Phys. Rev. C **75**, 024908 (2007)
- [24] T. Renk, J. Ruppert (2006)
- [25] G. Vujanovic, C. Young, B. Schenke, R. Rapp, S. Jeon et al., Phys. Rev. C **89**, 034904 (2014)
- [26] R. Ryblewski, M. Strickland (2015), arXiv: 1501.03418 [nucl-th]
- [27] C. Gale, Y. Hidaka, S. Jeon, S. Lin, J.F. Paquet et al. (2014), arXiv: 1409.4778
- [28] B. Schenke, C. Greiner, Phys. Rev. C **73**, 034909 (2006)
- [29] K. Schmidt, E. Santini, S. Vogel, C. Sturm, M. Bleicher, H. Stöcker, Phys. Rev. C **79**, 064908 (2009)
- [30] E. Bratkovskaya, W. Cassing, O. Linnyk, Phys. Lett. B **670**, 428 (2009)
- [31] O. Linnyk, E. Bratkovskaya, V. Ozvenchuk, W. Cassing, C. Ko, Phys. Rev. C **84**, 054917 (2011)
- [32] J. Weil, H. van Hees, U. Mosel, Eur. Phys. J. A **48**, 111 (2012)
- [33] E. Santini, J. Steinheimer, M. Bleicher, S. Schramm, Phys. Rev. C **84**, 014901 (2011)
- [34] S. Endres, H. van Hees, J. Weil, M. Bleicher, J. Phys. Conf. Ser. **503**, 012039 (2013)
- [35] S. Endres, H. van Hees, M. Bleicher, PoS **CPOD2013**, 052 (2013)
- [36] S. Endres, H. van Hees, J. Weil, M. Bleicher (2014), arXiv: 1412.2554 [nucl-th]
- [37] S. Endres, H. van Hees, J. Weil, M. Bleicher (2014), arXiv: 1502.01948 [nucl-th]
- [38] G. Agakishiev et al. (HADES Collaboration), Phys. Rev. C **84**, 014902 (2011)
- [39] G. Agakishiev et al. (HADES Collaboration), Eur. Phys. J. A **48**, 64 (2012)
- [40] O. Buss, T. Gaitanos, K. Gallmeister, H. van Hees, M. Kaskulov et al., Phys. Rept. **512**, 1 (2012)
- [41] J. Weil, U. Mosel, J. Phys. Conf. Ser. **426**, 012035 (2013)
- [42] J. Weil, S. Endres, H. van Hees, M. Bleicher, U. Mosel (2014), arXiv:1410.4206 [nucl-th]
- [43] J. Weil, S. Endres, H. van Hees, M. Bleicher, U. Mosel (2014), arXiv: 1412.3733 [nucl-th]
- [44] D. Manley, E. Saleski, Phys. Rev. D **45**, 4002 (1992)
- [45] S. Endres, H. van Hees, J. Weil, M. Bleicher (2015), work in progress
- [46] R. Rapp, J. Wambach, Eur. Phys. J. A **6**, 415 (1999)
- [47] H.J. Specht (NA60 Collaboration), AIP Conf.Proc. **1322**, 1 (2010)
- [48] R. Arnaldi et al. (NA60 Collaboration), Eur. Phys. J. C **61**, 711 (2009)
- [49] G. Brown, M. Rho, Phys. Rept. **269**, 333 (1996)
- [50] G. Brown, M. Rho, Phys. Rev. Lett. **66**, 2720 (1991)
- [51] C. Sasaki (2005)
- [52] M. Harada, C. Sasaki, Phys. Rev. D **73**, 036001 (2006)
- [53] A. Adare et al. (PHENIX Collaboration), Phys. Rev. C **81**, 034911 (2010)
- [54] H. van Hees, C. Gale, R. Rapp, Phys. Rev. C **84**, 054906 (2011)
- [55] H. van Hees, M. He, R. Rapp, Nucl. Phys. A **933**, 256 (2014)
- [56] R. Rapp, H. van Hees, M. He, Nucl. Phys. A **931**, 696 (2014)
- [57] R. Rapp, H. van Hees (2014), arXiv: 1411.4612 [hep-ph]